

Thermodynamics and kinetics of carbothermal reduction of zinc ferrite by microwave heating

Xin WANG^{1,2,3}, Da-jin YANG⁴, Shao-hua JU^{1,2,3}, Jin-hui PENG^{1,2,3}, Xin-hui DUAN^{1,2,3}

1. Faculty of Metallurgy and Energy Engineering, Kunming University of Science and Technology, Kunming 650093, China;

2. Key Laboratory of Unconventional Metallurgy, Ministry of Education, Kunming University of Science and Technology, Kunming 650093, China;

3. Engineering Laboratory of Microwave Application and Equipment Technology, Kunming 650093, China;

4. Kunming Metallurgy Research Institute, Kunming 650093, China

Received 21 September 2012; accepted 11 October 2013

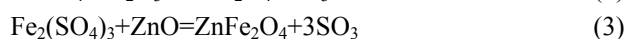
Abstract: The kinetics of carbon reduction of ZnFe_2O_4 in the temperature range of 550–950 °C was investigated in a microwave tank-type reactor. The mechanism of formation of ZnO and $\text{Fe}_3\text{O}_4/\text{FeO}$ by the decomposition of ZnFe_2O_4 was detailed using the equilibrium calculations and thermodynamics analysis by HSC chemistry software 6.0. In addition, the effects of decomposition temperature, the $\text{C}/\text{ZnFe}_2\text{O}_4$ ratio, the particle size and the microwave power were assessed on the kinetics of decomposition. Zn recovery as high as 97.93% could be achieved at a decomposition temperature of 750 °C with $\text{C}/\text{ZnFe}_2\text{O}_4$ ratio of 1:3, particle size of 61–74 μm and microwave power of 1200 W. The kinetics of decomposition was tested with different kinetic models and carbon gasification control mechanism was identified to be the appropriate mechanism. The activation energy for the carbon gasification reaction was estimated to be 38.21 kJ/mol.

Key words: zinc ferrite; activation energy; microwave; carbothermal reduction

1 Introduction

Zinc ferrite (ZnFe_2O_4), a kind of spinel, has a wide range of applications such as heterogeneous catalyst in H_2 production, semiconductor photocatalyst, gas sensor and photoelectron chemical cells. In hydrometallurgical processing of zinc, many insoluble materials such as zinc ferrite are concentrated in the leached residue. The leached residue contains a significant part of zinc in the form of zinc ferrite [1].

Zinc ferrites is a by-product of zinc processing industry, and it is mostly produced by the roast process of sphalerite or marmatite in the temperatures range from 800 to 1300 °C in an oxidizing atmosphere [2–4]. The possible reactions of zinc ferrite's formation are written as follows:



ZnFe_2O_4 is very stable as it doesn't dissolve in most acidic and alkaline medium, posing a serious problem for the hydrometallurgical recovery processes [5]. Generally high leaching temperature and acid concentration have been recommended to improve the zinc recovery [6–10]. However, it is well known to pyrometallurgical industry to decompose the zinc ferrite by carbon reduction [7]. When the carbon reduction is at temperatures higher than 1500 °C, the ZnFe_2O_4 breaks down into ZnO and $\text{Fe}_3\text{O}_4/\text{FeO}$ in Waelz kiln [11].

The decomposition of zinc ferrite was reported at 750 °C using carbon monoxide as reducing agent [12]. HUA et al [13] reported the formation of a mixture of Fe_3O_4 , FeO and zinc fume at 1000 °C. LIANG et al [14] reported the activation energy for reduction of ZnFe_2O_4 . However, references pertaining to the thermodynamics

and kinetics of ZnFe_2O_4 decomposition using microwave heating are sparse.

The conventional heating methods, typically heated from the hearth wall, do not ensure a uniform temperature of the material inside the furnace. This generates a temperature gradient from the hot surface of the sample particle to its interior, and impedes the effective removal of gaseous products to its surroundings, thereby resulting in long reaction time and higher energy consumption. Microwave heating is increasingly utilized in various technological and scientific fields for variety of applications, due to its advantage of faster and uniform heating rate as compared to conventional heating method. The energy transfer is not affected by conduction or conventional heating, but is readily transformed into heat inside the particles by dipole rotation and ionic conduction. When high frequency voltages are applied to a material, the response of the molecules with a permanent dipole to the applied potential field is to change their orientation in the direction opposite to that of the applied field, which causes the molecules to agitate and generate heat. The tremendous temperature gradient from the interior of the char particle to its cool surface allows the microwave induced reaction to proceed more quickly and effectively, resulting in energy saving and shorter reaction time. [15–17].

In the present work, the Equilibrium Module of HSC Chemistry 6.1 is used to analyze the decomposition of zinc ferrite [18]. In addition, the kinetics of microwave decomposition of ZnFe_2O_4 along with the effect of the various parameters on the kinetics is presented.

2 Experimental

2.1 Materials

The zinc residues used for the experiments were supplied by a metallurgical plant of Yunnan province, China. Prior to use the samples were washed, dried and sieved to different size ranges for experiments. X-ray diffraction analysis (XRD) of the zinc residue to assess the mineralogical structure is presented in Fig. 1.

XRD analysis showed the presence of zinc ferrite (ZnFe_2O_4), lead sulfate (PbSO_4) and quartz (SiO_2) as the major components in plant residues. The chemical composition and particle size distribution of the zinc residues, were analyzed and listed in Table 1.

2.2 Method

The zinc ferrite sample and carbon were mixed at a desired C/ ZnFe_2O_4 ratio and the mixture was heated to a desired temperature in a microwave tank-type reactor,

having a frequency of 2.45 GHz and a maximum output power of 3 kW. The schematic of the experimental facility is shown in Fig. 2.

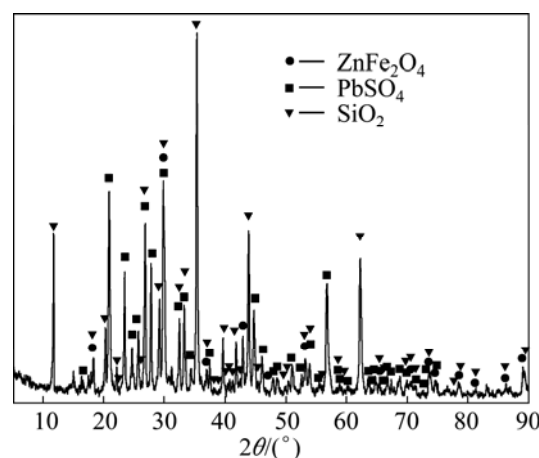


Fig. 1 XRD pattern of zinc plants residue

Table 1 Chemical analysis of different sieve fractions of zinc residues

No.	Size/ μm	Content/%	Element content/%			
			Zn	Fe	Pb	SiO_2
1	104–89	11	12.68	21.22	12.26	6.99
2	89–74	13	12.80	20.36	12.38	6.95
3	74–61	19	12.48	21.75	12.50	7.03
4	61–53	21	12.36	21.64	12.19	7.00
5	<53	36	12.58	21.15	12.07	7.10

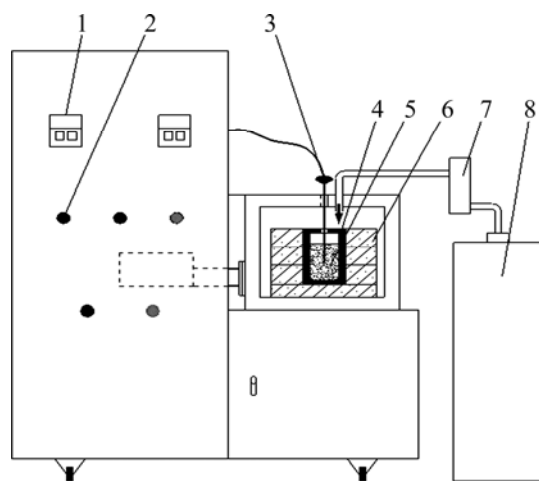


Fig. 2 Schematic of experimental set-up: 1—Instrument display; 2—Controller; 3—Thermocouple; 4—Crucible; 5—Experimental material; 6—Heat preservation material; 7—Flowmeter; 8—Nitrogen vessel

The temperature in furnace was measured using a chrome-nickel silicon armor type couple with the temperature range of 0 to 1250 °C, which was controlled with a single mode continuous controllable power. The

samples were heated to the desired temperature, with the N_2 flow rate of $150 \text{ cm}^3/\text{min}$. The desired temperature could be achieved within a short duration of less than 5 min, which clearly indicates the effectiveness of microwave heating system. The experiments were conducted covering the process parameters of reaction temperature of $550\text{--}950^\circ\text{C}$, $C/\text{ZnFe}_2\text{O}_4$ ratio of $1/6$ to 1 and the microwave power of $600\text{--}2400 \text{ W}$.

In order to assess the degree of decomposition of ZnFe_2O_4 , the liberation of zinc was performed by leaching the zinc with sulfuric acid at a leaching temperature of 65°C , sulfuric acid concentration of 170 g/L , particle size of $53\text{--}61 \mu\text{m}$ and solid-to-liquid of $4:1$.

2.3 Kinetics analysis

Solid heterogeneous reactions have number of applications in chemical and pyrometallurgy processes. In order to determine the kinetic parameters and the rate controlling step for the decomposition of Zinc ferrite, the experimental data were analyzed using popular kinetic models [19].

In these types of reaction, the reaction rate may be usually controlled by reaction or by diffusion through the product layer or by the chemical reaction at the surface of the material.

If the reaction is controlled by carbon gasification control, it will have an integrated rate equation as follows:

$$\ln(1 - m_{c,\text{close}}/m_{c,0}) = -kt \quad (4)$$

If the reaction is controlled by chemical reaction on the surface then

$$1 - (1 - a)^{1/3} = kt \quad (5)$$

If the reaction is controlled by diffusion through the product layer then

$$[1 - (1 - a)^{1/3}]^2 = kt \quad (6)$$

$$1 - 2/3a - (1 - a)^{2/3} = kt \quad (7)$$

where $m_{c,0}$ is the mass of initial carbon; $m_{c,\text{close}}$ is the mass of consumed carbon; a is the fraction reacted; k is the kinetic parameter for reaction control; t is the reaction time (min). Eqs. (4–7) show that there must be a linear relationship between the left side of the equations and t . The slope of the line is the rate constant k , also the temperature dependence of the reaction rate constant can be calculated by the Arrhenius equation as follows:

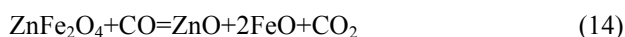
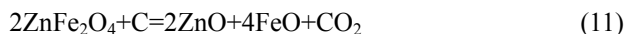
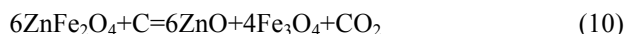
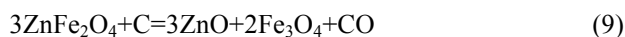
$$k_d = A \exp\left(\frac{-E_a}{RT}\right) \quad (8)$$

where A is frequency factor; E_a is the activation energy of the reaction; R is the gas constant and T is temperature.

2.4 Reaction mechanics and thermodynamics

The different species and phases, which were known to be existing, were specified into the reaction equation box of HSC software [20] with the ability to calculate multi-component equilibrium compositions for the heterogeneous systems. The heat capacity, enthalpy, entropy and Gibbs energy of a single species and reactions system between pure substances can also be estimated through the HSC software [18].

Although the thermodynamic properties of zinc ferrite were well-established, the thermodynamic data pertaining to carbon reduction were not available [18]. Carbon reduction was usually carried out at high temperature using a reducing agent. The process of ZnFe_2O_4 decomposition can be described by the following reactions:



The Gibbs free energy change (ΔG) of the reactions (9–14) can be calculated using the reaction equations module of HSC. The effects of temperature on the ΔG of the reactions (9–14) are shown in Fig. 3.

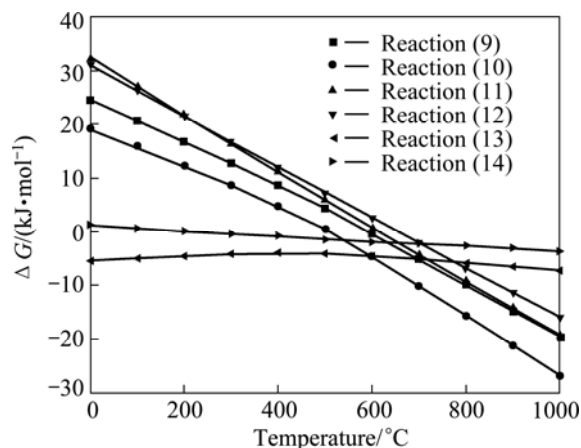


Fig. 3 Variation of ΔG with temperature for reactions (9–14)

As shown in Fig. 3, only reactions (13) and (14) seem to be favorable to drive the reaction to the right at low temperatures and it doesn't show any variation with increase of temperature. The extent to which the reaction was driven to the right can also be inferred from the magnitude of the ΔG . Both reactions (13) and (14) relate to zinc ferrite reaction with CO. Reactions (9–12) can't be driven to product at low temperatures, while can be driven to the right resulting in significant yields beyond a

temperature of 600 °C. Reaction (10) seems to be favorable as compared to the other reactions as the shift from the positive ΔG to negative ΔG occur at temperature around 500 °C

Substituting the compounds, such as ZnFe_2O_4 , ZnO , Fe_3O_4 , FeO , C , CO and CO_2 , into the equilibrium module of HSC chemistry 6.1 generates a list of 58 species. Since most of the species are unstable, only 8 species involving 3 phases were utilized in the calculations are gases: N_2 , CO , CO_2 ; oxides: FeO , Fe_3O_4 , ZnFe_2O_4 , ZnO and carbon.

The behaviors of all the listed species as a function of temperature are shown in Fig. 4.

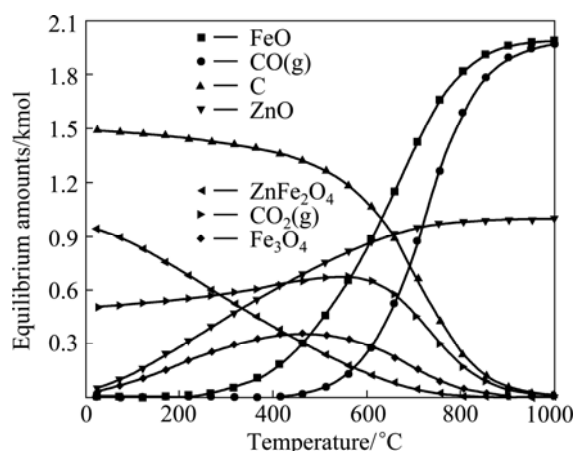


Fig. 4 Effect of temperature on equilibrium amounts

Carbon, zinc ferrite and a small amount of gaseous CO_2 were the most significant species at the beginning of the carbon reduction reaction. The zinc ferrite begins to decompose at about 600 °C, and decomposition degree increases with increasing of temperature. A further increase of reaction temperature results in ZnFe_2O_4 being consumed with the vigorous formation of FeO and ZnO . The formation of FeO was also contributed by the reduction of Fe_3O_4 in the reducing atmosphere. The amount of CO increases somewhat with temperature, while the amount of carbon decreases. The above results indicate the favorable decomposition temperature for the zinc ferrite was a temperature in excess of 600 °C, which forms the theoretical basis for the further kinetic study.

The effects of temperature on the equilibrium composition of the decomposition of zinc ferrite with carbon and without carbon were shown in Figs. 5 and 6. Figure 5 shows the similar decomposition behaviors as in Fig. 4, except that the C , CO , CO_2 were removed as they were insignificant. Figure 5 shows only a 50% decomposition of zinc ferrite at temperature as high as 2500 °C, clearly indicating the difficulty of thermal decomposition and confirming the favorable decomposition conditions using carbon reduction.

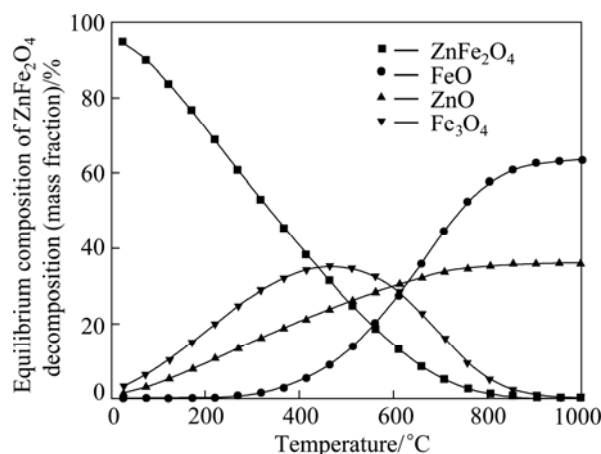


Fig. 5 Effect of temperature on equilibrium composition of zinc ferrite decomposition with carbon

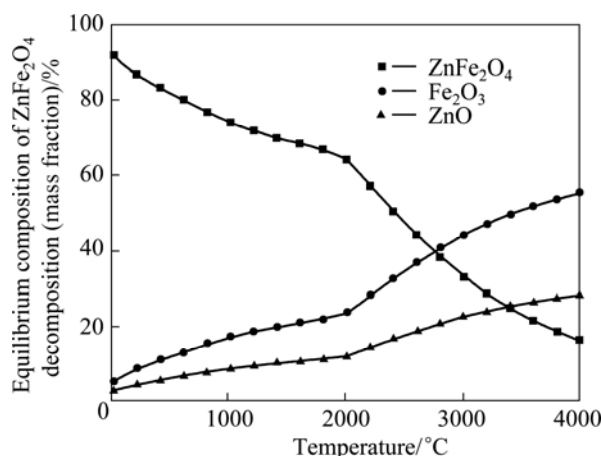


Fig. 6 Effect of temperature on equilibrium composition of zinc ferrite decomposition without carbon

3 Results and discussion

The effects of reaction temperature, ratio of $\text{C}/\text{ZnFe}_2\text{O}_4$, particle size and microwave power on the carbon reduction of ZnFe_2O_4 were assessed.

3.1 Effects of reaction temperature

The influence of temperature on the decomposition of ZnFe_2O_4 , indicated in the form of Zn recovery, is shown in Fig. 7 with the other parameters holding at $\text{C}/\text{ZnFe}_2\text{O}_4$ of 1:3, particle size of 61–74 μm and microwave power of 1200 W. The results indicate that temperature has a major role on the zinc ferrite decomposition process.

Figure 8 shows the XRD patterns of reduction product at different temperature. When the decomposition temperature exceeded 650 °C, the decomposition products of zinc ferrite as Fe_3O_4 , FeO , ZnO appeared. As expected, zinc ferrite decomposition degree increased with the increase of temperature, the Zn

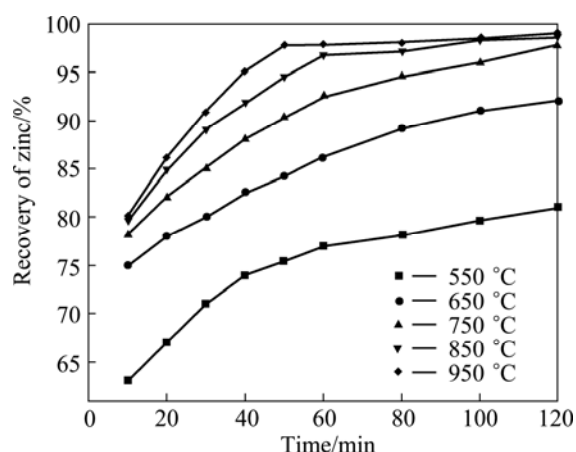


Fig. 7 Effect of reaction temperature on decomposition of zinc ferrite

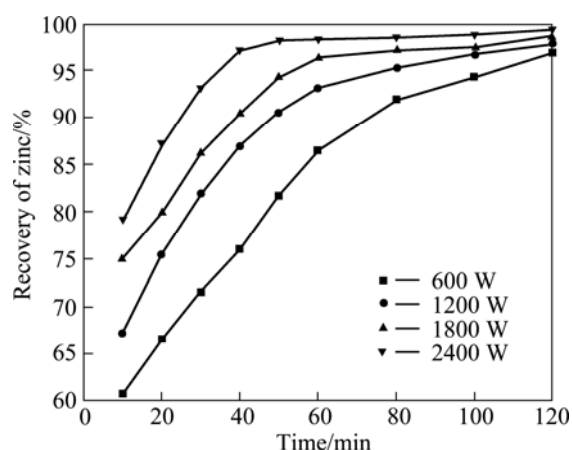


Fig. 9 Effect of microwave power on decomposition of zinc ferrite

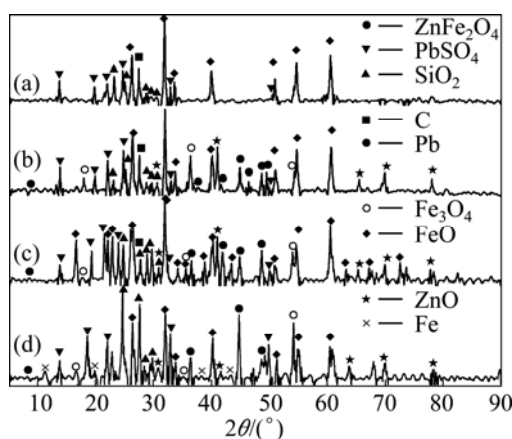


Fig. 8 XRD patterns of microwave heating reduction products at different temperature: (a) 550 °C; (b) 650 °C; (c) 750 °C; (d) 850 °C

recovery increased from 74% to 97% when the temperature increased from 550 to 950 °C. However, a significant slow down of the recovery of zinc in the final stage was noted, owing to the near completion of the reaction. The high recovery can be attributed to the microwave's capability to heat the materials in molecular level.

3.2 Effects of microwave power

The recoveries of zinc with the increase of the microwave power under constant conditions of reaction temperature of 750 °C, C/ZnFe₂O₄ ratio of 1:3, particle size of 61–74 μm are shown in Fig. 9.

The results show that the rate of recovery increased with increase of microwave power. At higher microwave power, the ability of the microwave to heat to the set temperature of 750 °C could be achieved at a much faster rate, and hence driving the carbon reaction to completion at a much faster rate. The reaction could be driven to near completion within a duration of 40 min at a power

input of 2400 W as compared with a duration in excess of 120 min at a power input of 600 W.

3.3 Effects of particle size

The influence of particle size on the zinc ferrite decomposition was examined using five different particle sizes (89–104 μm, 74–89 μm, 64–74 μm, 53–61 μm and <53 μm), with the other parameters holding at a reaction temperature 750 °C, C/ZnFe₂O₄ ratio of 1:3 and microwave power of 1200 W is shown in Fig. 10.

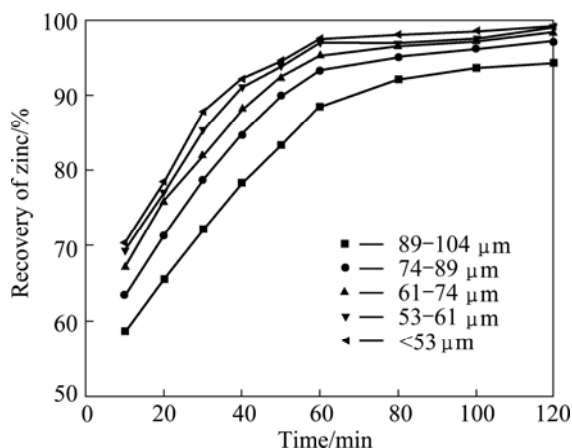


Fig. 10 Effect of particle size on decomposition of zinc ferrite

The results indicate that the smaller the particle size was, the faster the degree of decomposition of zinc was. The smaller particle size could facilitate faster heating, as well as increase of the rate of the carbon reaction due to the high surface area of contact between the zinc ferrite and the carbon particles. However, a significant increase of the Zn recovery was observed in a particle size range of 61–74 μm.

3.4 Effects of ratio of C/ZnFe₂O₄

The C/ZnFe₂O₄ ratio was examined in the range of

1:1 to 1:6, with the decomposition reaction temperature of 750 °C, particle size of 150–270 μm and microwave power of 1200 W.

As seen from Fig. 11, the effect of C/ZnFe₂O₄ ratio on the decomposition of zinc ferrite increases with increase of C/ZnFe₂O₄ ratio, which indicated increase of zinc recovery. Significant improvement in the Zn recovery was observed only at C/ZnFe₂O₄ in excess of 1:3. At low ratio's (high ferrite), the availability of the carbon for the carbon reaction could be limiting, hence limiting the conversion of the carbon reaction. In other words, it could be due to the availability of carbon less than the stoichiometric requirement of the carbon reaction. At high ratio's, the availability of carbon in excess of the stoichiometric requirement doesn't contribute to the increase in the extent of reaction.

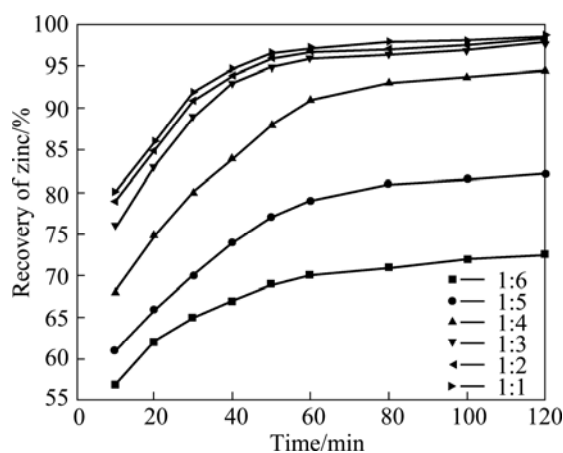


Fig. 11 Effect of C/ZnFe₂O₄ ratio on decomposition of zinc ferrite

3.5 Kinetics of decomposition reaction

The kinetics of the decomposition of zinc ferrite was tested with different model equations as detailed in section 2.3 to identify the rate controlling step. Equations. (4–7) were fitted with the experimental kinetic data, as shown in Figs. (12–15), to identify the rate controlling step.

The appropriateness of the model equation in representing the experimental data was estimated with the regression coefficient (R^2). All the models were found to match the experimental data very well at temperatures higher than 823 K, which clearly indicates that making a choice of an appropriate model based on the fit of the experimental data could be misleading. The results show that the straight lines with the regression coefficient R^2 in Fig. 13 are closer to 1 than others. And the experimental data pertaining to the temperature of 823 K clearly indicates that the reaction was carbon gasification controlled. So Eq. (4) was found to fit the data best, and the carbon gasification control model was identified to be an appropriate model, which was utilized

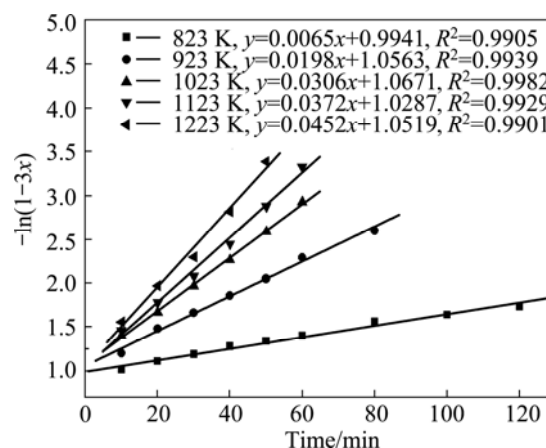


Fig. 12 Variation of $-\ln(1-3x)$ with time at various temperatures

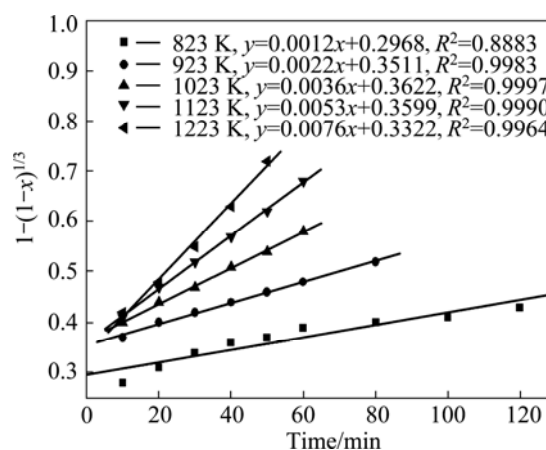


Fig. 13 Variation of $1-(1-x)^{1/3}$ with time at various temperatures

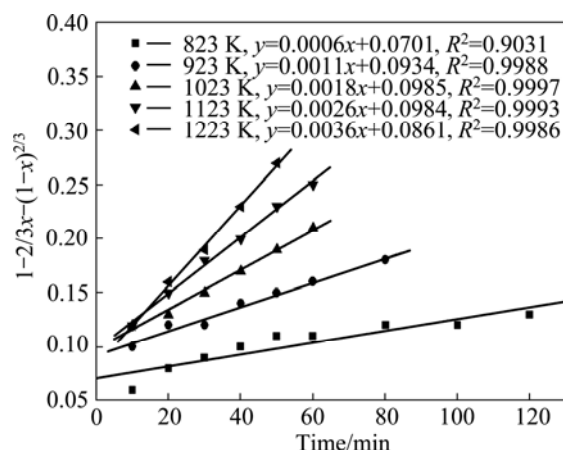


Fig. 14 Variation of $1-(2/3)x-(1-x)^{2/3}$ with time at various temperatures

for the estimating of the activation energy for the reaction.

The activation energy, for the zinc ferrite decomposition reaction was estimated with the use of Arrhenius plot. The frequency factor and the activation

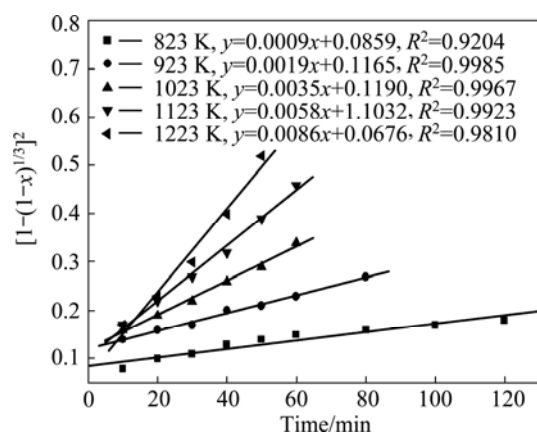


Fig. 15 Variation of $[1-(1-x)^{1/3}]^2$ with time at various temperatures

energy were estimated from the slope and intercept of the plot of $\ln k$ versus $1/T$, where T was in the range of 550 to 950 °C. The activation energy of decomposition on zinc ferrite was estimated to be 38.21 kJ/mol.

4 Conclusions

1) The thermodynamics mechanism of the formation of ZnO and $\text{Fe}_3\text{O}_4/\text{FeO}$ by the decomposition of ZnFe_2O_4 can be explained by the equilibrium calculations and thermodynamics analysis using HSC chemistry software 6.0.

2) Based on the thermodynamic calculation, the temperature in the range of 550–950 °C can be determined. For the carbon composition used, the thermodynamic equilibrium shows that zinc ferrite begins to decompose difficultly without reduction condition, the amount of decomposed zinc ferrite barely reaches 50% at 2500 °C. So, the carbon reduction could help to decrease the reaction temperature.

3) The parameters used in the decomposition kinetics experiments, such as the effects of temperature, the ratio of $\text{C}/\text{ZnFe}_2\text{O}_4$, particle size and microwave power on the kinetics of decomposition of Zinc ferrite were investigated. The results show that the optimum leaching conditions were determined as reaction time 120 min, reaction temperature 750 °C, $\text{C}/\text{ZnFe}_2\text{O}_4$ ratio 1:3, particle size of 61–74 μm and microwave power of 1200 W, under which 97.93% of zinc was recovered.

4) The kinetic data for decomposition of ZnFe_2O_4 show a good fit to $\ln(1-m_{\text{c,loss}}/m_{\text{c,0}}) = -kt$, and the reaction rate was controlled by the carbon gasification control kinetic model. The activation energy was calculated to be 38.21 kJ/mol.

References

[1] TURAN M D, ALTUNDOG H S, TQMEN F. Recovery of zinc and

lead from zinc plant residue [J]. Hydrometallurgy, 2004, 75: 169–176.

[2] SINCLAIR W D, KOOIMAN G J A, MARTIN, D A, KJARSGAARD I M. Geology, geochemistry and mineralogy of indium resources at Mount Pleasant, New Brunswick, Canada [J]. Ore Geology Reviews, 2006, 28: 123–145.

[3] TONG X, SONG S X, HE J, LOPEZVALDIVIESO A. Flotation of indium-bearing, marmatite from multi-metallic ore [J]. Rare Metals, 2008, 27: 107–111.

[4] GRAYDON J W, KIRK D W. The mechanism of ferrite formation from iron sulfides during zinc roasting [J]. Metallurgical and Materials Transactions B, 1988, 19: 777–785.

[5] ZHANG Y J, LI X H, PAN L P, LIANG X Y, LI X P. Studies on the kinetics of zinc and indium extraction from indium-bearing zinc ferrite [J]. Hydrometallurgy, 2010, 100: 172–176.

[6] North-east Institute of Technology. Zinc Metallurgy [M]. Beijing: Metallurgical Industry Press, 1974: 29–31. (in Chinese)

[7] XU C D, LIN R, WANG D C. Physical chemistry for zinc metallurgy [M]. Shanghai: 3ed, Shanghai Scientific and Technological Press, 1979. (in Chinese)

[8] HAVLÍK T, FRIEDRICH B, STOPIC S. Pressure leaching of EAF dust with sulphuric acid [J]. Erzmetall, 2004, 57: 113–120.

[9] FILIPPOU D, DEMOPOULOS G P. On the various dissolution kinetics of zinc ferrite in acid media [J]. Canadian Journal of Chemical Engineering, 1993, 71: 790–801.

[10] FILIPPOU D, DEMOPOULOS G P. A reaction kinetic model for the leaching of industrial zinc ferrite particulates in sulfuric acid media [J]. Can Metall Q, 1992, 31: 41–54.

[11] MATSUNO M, OJIMA Y, KAIKAKE A. EAF dust treatment operation at Sumitomo Shisaka works [C]//Symposium on Extraction and Applications of Zinc and Lead. Japan, 1995: 432–441.

[12] NYIRENDA R L. An appraisal of the carbon zinc process when zinc ferrite is reduced to a magnetite containing product [J]. Minerals Engineering, 1990, 3: 319–329.

[13] HUA P, PAN D A, WANG X F, TIAN J J, WANG J, ZHANG S G, VOLINSKY A A. Fuel additives and heat treatment effects on nanocrystalline zinc ferrite phase composition [J]. Journal of Magnetism and Magnetic Materials, 2011, 323(5): 569–573.

[14] LIANG M S, KANG W K, XIE K C. Comparison of reduction behavior of Fe_2O_3 , ZnO and ZnFe_2O_4 by TPR technique [J]. Journal of Natural Gas Chemistry, 2009, 18: 110–113.

[15] YAGMUR E, OZMAK M, AKTAS Z. A novel method for production of activated carbon from waste tea by chemical activation with microwave energy [J]. Fuel, 2008, 87: 3278–3285.

[16] HUANG Z C, WU K, HU B, PENG H, JIANG T. Non-isothermal kinetics of reduction reaction of oxidized pellet under microwave irradiation [J]. Journal of Iron and Steel Research, International, 2012, 19: 1–4.

[17] PICKLES C A. Microwave heating behavior of nickeliferous limonitic laterite ores [J]. Minerals Engineering, 2004, 17: 775–784.

[18] PICKLES C A. Thermodynamic modelling of the formation of zinc-manganese ferrite spinel in electric arc furnace dust [J]. Journal of Hazardous Materials, 179: 309–317.

[19] HAN Q Y. Kinetics of reactions in metallurgical processes [J]. Beijing: Metallurgical Industry Press, 1983.

[20] FENG B, BHATIA S K. On the validity of thermogravimetric determination of carbon gasification kinetics [J]. Chemical Engineering Science, 2002, 57: 2907–2920.

微波加热碳热还原铁酸锌的动力学及热力学

王 欣^{1,2,3}, 杨大锦⁴, 巨少华^{1,2,3}, 彭金辉^{1,2,3}, 段昕辉^{1,2,3}

1. 昆明理工大学 冶金与能源工程学院, 昆明 650093;

2. 昆明理工大学 非常规冶金教育部重点实验室, 昆明 650093;

3. 微波能工程应用及装备技术国家地方联合工程实验室, 昆明 650093;

4. 昆明冶金研究院, 昆明 650093

摘 要: 研究 550–950 °C 下微波加热配碳还原焙烧分解铁酸锌生成 ZnO 和 Fe₃O₄/FeO 的工艺及机理。利用 HSC 热力学软件对铁酸锌分解的热力学温度进行计算, 并利用碳气化控制、化学控制及扩散控制模型研究样品中铁酸锌分解的动力学行为。分析微波功率、反应温度、配碳比和时间对铁酸锌分解率的影响。结果表明: 在微波加热温度 750 °C, C/ZnFe₂O₄ 质量比为 1:3, 粒径 74–89 μm, 微波功率 1.2 kW 的条件下, 被还原的铁酸锌样品经过浸出后, Zn 的回收率可以高达 97.93%。通过采用不同的动力学模型对分解动力学进行测试。结果表明: 碳气化控制机制是良好的机制。碳气化反应的活化能为 38.21 kJ/mol。

关键词: 铁酸锌; 活化能; 微波加热; 碳热还原

(Edited by Chao WANG)